Analysis of the TPS Gene Family and Functional Characterization of Rust Resistance in Zanthoxylum armatum DC

Yingming Lai
Sichuan Agricultural University
Xingyu Liu
Sichuan Agricultural University
Li Zhao
Sichuan Agricultural University
Tianhui Zhu
Sichuan Agricultural University
Shujiang Li
Sichuan Agricultural University
Shuying Li
Sichuan Agricultural University
Meng Ye
Sichuan Agricultural University
Chunlin Yang
Sichuan Agricultural University
Yujue Zhou
Sichuan Agricultural University
Shan Han
hanshan6618@163.com
Sichuan Agricultural University

Research Article

Keywords: Zanthoxylum armatum, Rust resistance, Linalool, Transient expression

Posted Date: August 5th, 2026

DOI: https://doi.org/10.21203/rs.3.rs-10588166/v1

Additional Declarations: No competing interests reported.

Analysis of the TPS Gene Family and Functional Characterization of Rust Resistance in *Zanthoxylum armatum* DC

Yingming Lai[1], Xingyu Liu[1+], Li Zhao[1],Tianhui Zhu [1,2]， Shuying Li[1], Shujiang Li[1], Meng Ye[1*], Chunlin Yang[1,2], Yujue Zhou[1], Shan Han[1,2*]

[1]College of Forestry, Sichuan Agricultural University, Chengdu, Sichuan Province, 611130, P.R. China

[2]Key Laboratory of Forest Protection of Sichuan Education Department, Chengdu, Sichuan Province, 611130, P.R. China

*Corresponding author:Shan Han; E-mail address: hanshan6618@163.com; 13722@sicau.edu.cn

Highlights:

• *ZaTPS* was cloned and functionally characterized from *Zanthoxylum armatum* for the first time;

• Overexpression of *ZaTPS* significantly enhances linalool accumulation and directly inhibits rust spore germination.

• *ZaTPS* enhances antioxidant defense capacity, reducing oxidative damage during rust infection.

• Silencing of *ZaTPS* increases susceptibility to rust, confirming its role as a positive regulator of disease resistance.

Abstract

Background

Zanthoxylum armatum is an economically important spice and medicinal plant whose industry is often severely threatened by rust disease. To investigate the role of the terpene synthase (TPS) gene in rust resistance, the *ZaTPS* gene (1206 bp) was cloned from the resistant cultivar 'Youkang'.

Results

Bioinformatics analysis revealed that it encodes an acidic, hydrophilic protein

localized to the cytoplasm, lacking a signal peptide and transmembrane domains. Tissue-specific expression analysis showed that *ZaTPS* transcript levels were significantly higher in resistant plants and in leaves compared to susceptible ones. Transient overexpression and silencing of *ZaTPS* were successfully achieved in *Z. armatum* via *Agrobacterium*-mediated transformation. Functional studies demonstrated that overexpression of *ZaTPS* significantly increased the content of a key terpenoid (linalool) in leaves and effectively inhibited the germination of rust spores. Concurrently, the expression of pivotal genes in the terpenoid biosynthesis pathway (e.g., DXP, DXR, IPP) was significantly upregulated in overexpression plants. Following rust inoculation, plants overexpressing *ZaTPS* exhibited significantly lower disease incidence and severity index compared to controls, indicating enhanced resistance, whereas silenced plants showed increased susceptibility. Furthermore, *ZaTPS* expression positively regulated the activities of antioxidant enzymes (CAT, SOD, POD) and reduced the accumulation of malondialdehyde (MDA), thereby bolstering cellular defense capacity.

Conclusions

Overall, *ZaTPS* plays a crucial positive regulatory role in the rust resistance of *Z. armatum* by promoting terpenoid (particularly linalool) biosynthesis and enhancing the antioxidant defense system. This study provides important theoretical foundations for elucidating the molecular mechanisms of rust resistance in *Z. armatum* and for breeding new resistant cultivars.

Keywords:*Zanthoxylum armatum* ; Rust resistance ; Linalool ; Transient expression

1.Background

Zanthoxylum armatum DC., a plant species within the genus *Zanthoxylum* of the Rutaceae family, has a long history of cultivation in China[1].Its unique flavor profile and applications in medicinal and preservative contexts have led to a flourishing industry, bringing increasing attention to its economic and ecological value[2-3].However, the growth and development of *Z. armatum* are susceptible to pest

and disease infestations, which can severely impact its economic worth[4].Common diseases and pests affecting *Z. armatum* include rust, root rot, anthracnose, aphids, and spider mites.Among these, rust disease stands out as the most prevalent and damaging across major cultivation regions[5-8].This disease significantly disrupts normal plant development, drastically reduces fruit set, and consequently leads to substantial yield losses[9].Surveys indicate widespread occurrence of rust disease with varying severity in most *Z. armatum* production areas of Sichuan Province, posing a serious constraint to the sustainable development of the industry[10].

Current research primarily focuses on the epidemiology of rust, the biological characteristics of the pathogen, and the isolation and identification of hyperparasitic fungi, while knowledge regarding the function of host resistance genes in *Z. armatum* itself remains limited.Therefore, controlling rust disease is essential to ensure the healthy growth and guaranteed yield of *Z. armatum* and to support a thriving market.Studies have revealed significant variation in rust resistance among different *Z. armatum* cultivars[11-13].Presently, control strategies for rust are underdeveloped, with chemical applications remaining the primary method during disease outbreaks[14-15].Although chemical control can suppress the disease, its associated environmental pollution and hazards to biodiversity are significant concerns in the context of green and sustainable pest management[16-17].Inspired by the success in staple crops like wheat and maize where screening for resistant genotypes has been a key strategy for combating pathogens[18-20], and building upon the prior identification of a resistant cultivar ('Youkang') and a susceptible cultivar ('Tengjiao') by our research group, this study aims to investigate and functionally characterize key rust resistance genes in *Z. armatum*.

Plant secondary metabolic pathways play crucial roles in coping with adverse environments, resisting pathogenic microorganisms, and promoting plant morphological differentiation through the synthesis of diverse compounds[21-22].Based on their chemical structures, plant secondary metabolites can be categorized into terpenoids, phenolics, nitrogen-containing compounds, and others.Among these, terpenoids constitute the largest and most diverse group[23-24].Terpenes are widely

used in commercial perfumes and food additives and exhibit a broad spectrum of biological activities as pharmaceuticals, ranging from regulating human physiology (e.g., steroid hormones, cannabinoids) to treating diseases (e.g., paclitaxel, artemisinin)[25].The biosynthesis of terpenes primarily relies on terpene synthases (TPS), which catalyze the formation of monoterpene, sesquiterpene, diterpene, and polyterpene backbones[26].Transcriptional regulation of TPS gene expression is critical for modulating terpene biosynthesis.For instance, in grape, 22 genes of the MEP pathway, along with members of multiple transcription factor families, including bHLH, and several genes related to hormone biosynthesis or signaling, might participate in regulating terpenoid biosynthesis based on their specific expression patterns in berries[27].

Using the *Z. armatum* genome assembly, a local BLAST database was constructed.Local BLAST screening was performed using TPS sequences from *Arabidopsis thaliana* and *Citrus* as query sequences.This screening identified the gene model Zardc21150.t1, which was designated *ZaTPS*.The gene function of *ZaTPS* was investigated using RNA interference (RNAi) and overexpression techniques, aiming to analyze its role in terpene biosynthesis in *Z. armatum*.This research seeks to further elucidate the molecular mechanisms underlying rust resistance in *Z. armatum*.

2. Materials and Methods

2.1 Plant Materials

Two-year-old seedlings of *Zanthoxylum armatum* with uniform growth were selected for the experiment.The susceptible cultivar was 'Tengjiao' and the resistant line was 'Youkang'.All plants were cultivated in a greenhouse located at the Fifth Teaching Building of Sichuan Agricultural University in Wenjiang District, Chengdu.For subcellular localization assays, one-month-old *Nicotiana benthamiana* plants were used for transient transformation.

The inoculum source, urediniospores of the rust fungus *Coleosporium zanthoxyli* Diet.et Syd., was collected from diseased plants and stored at -80°C.

Plasmid vectors and microbial strains used included: the RNAi intermediate vector pHANNIBAL (Miaoling Bio), the plant expression vector pCAMBIA1300-35SN, the plant overexpression vector BG Plant-Express MCS (Baoguang Bio), and the transient expression vector pSuper 1300-GFP containing a GFP tag.Escherichia coli strain DH5α and *Agrobacterium* tumefaciens strain GV3101 were used for cloning and plant transformation, respectively.

2.2 Instruments and Reagents

Key instruments utilized in this study were: SW-CJ-2FD clean bench (Sujing Antai), DYY-6D electrophoresis apparatus (Beijing Liuyi Instrument Factory), pipettes (Gilson and Eppendorf), Vilber 3000 gel imaging system, CFX96Touch real-time PCR detection system, HZQ-F160 incubator shaker (HDL Apparatus), HH-6 constant temperature water bath (AHYQ), Mastercycler Gradient thermal cycler (Eppendorf), NanoPhotometer® N60 microvolume spectrophotometer (Implen), GZ-380-GSI intelligent artificial climate chamber, LDZX-40BI vertical autoclave, XW-80A vortex mixer (Vortex), centrifuge 5415R (Eppendorf), high-speed refrigerated centrifuge, JP-A platform balance (Lineng), JA3003 electronic balance (Liangping), and CV200 vacuum concentrator (Ningbo SCIENTZ).

Major reagents consisted of: SteadyPure Plant RNA Extraction Kit, SteadyPure Plant Genomic DNA Extraction Kit, Evo M-MLV Reverse Transcription Premix, and SYBR® Green Pro Taq HS Premixed qPCR Kit (all from Accurate Biotechnology); SanPrep Column PCR Product Purification Kit (Sangon Biotech); pEASY®-T5 Zero Cloning Kit, 2×EasyTaq® PCR SuperMix, and 2×TransTaq® High Fidelity (HiFi) PCR SuperMix II (TransGen Biotech); Plasmid Mini Preparation Kit (Biomed); restriction enzyme BamHI (Thermo Scientific); and Uniclone One Step Seamless Cloning Kit (Jinsha Biotechnology).

2.3 Total RNA Extraction and cDNA Synthesis

Fresh young leaves from resistant and susceptible plants were collected for total RNA extraction using the SteadyPure Plant RNA Extraction Kit (Accurate Biotechnology), following the manufacturer's protocol (available at:

https://agbio.com.cn/wp-content/uploads/2024/08/UM_AG21040-Version-1.pdf).RNA integrity was assessed by 1% agarose gel electrophoresis (140 V, 400 mA, 18 min), visualized under a gel imaging system.RNA concentration and purity were measured using a microvolume spectrophotometer.

High-quality total RNA was reverse-transcribed into first-strand cDNA using the 5X All-In-One RT MasterMix (abm), according to the manufacturer's instructions.The resulting cDNA was used for subsequent amplification of *ZaTPS* genes and expression analysis.The reaction components are listed in Table 1.

Table 1 cDNA TransScription System

Component	Volume
All-In-One 5X RT MasterMix	4 μL
RNA template	2 μL
Nuclease-Free Water	14 μL
Gently mix well; React on a PCR instrument	
Enzyme incubation	37℃ 30min
Reverse transcription	60℃ 10min
Termination reaction	95℃ 3min

2.4 Cloning and Bioinformatics Analysis of *ZaTPS*

The coding sequence (CDS) of *ZaTPS* was amplified from *Z. armatum* using specific primers designed based on the Zardc14604.t1 sequence retrieved from the *Z. armatum* genomic database (The chromosome-level genome assembly of Sichuan pepper).Sequence data were analyzed and aligned using DNAMAN with default parameters.A phylogenetic tree was constructed using the maximum likelihood (ML) method in TBtools with 1000 bootstrap replicates to ensure node reliability.

Physicochemical properties of the deduced *ZaTPS* protein, including theoretical isoelectric point (pI), molecular weight (MW), and grand average of hydropathicity (GRAVY), were predicted using the ProtParam tool on the Expasy server (http://web.expasy.org/protparam/).Signal peptide prediction was performed with SignalP 6.0 (https://services.healthtech.dtu.dk/services/SignalP-6.0/).Transmembrane helix prediction was conducted using TMHMM-2.0 (https://services.healthtech.dtu.dk/services/TMHMM-2.0/).Subcellular localization was predicted using WoLF PSORT (https://www.genscript.com/wolf-psort.html).

2.5 Tissue-specific Expression Pattern Analysis

Root, stem, and leaf tissues were collected from healthy, uniformly growing plants of the resistant 'Youkang' line and the susceptible 'Tengjiao' cultivar for *ZaTPS* expression analysis.Three biological replicates were performed for each sample.Total RNA was extracted from all samples, followed by first-strand cDNA synthesis and quantitative real-time PCR (qRT-PCR) analysis.The Actin gene was used as an internal reference for normalizing relative gene expression.

2.6 Subcellular Localization

The subcellular localization vector pCAMBIA1300-EGFP-MCS was linearized using the KpnI restriction site.Specific primers containing homologous arms flanking the linearized vector were designed to amplify the *ZaTPS* CDS, generating a *ZaTPS*-GFP recombinant construct.The recombinant plasmid and the empty vector control were introduced into *Agrobacterium* tumefaciens strain GV3101 competent cells using the liquid nitrogen freeze-thaw method.After 48 hours of culture, single colonies were selected and screened by colony PCR using specific primers to confirm successful transformation of the *ZaTPS*-GFP recombinant plasmid.Primers targeting the Kanamycin resistance region were used to verify the empty pCAMBIA1300-EGFP-MCS vector.

Agrobacterium cultures confirmed as positive were transferred to LB liquid medium containing Kanamycin and incubated overnight at 28°C with shaking at 200 rpm.When the OD600 reached 0.8-1.0, the cells were pelleted by centrifugation at 3000 rpm for 1 min.The pellet was resuspended in infiltration buffer (containing 10 mM MES, 10 mM $MgCl_2$, and 100 μM acetosyringone) and adjusted to a final OD600 of 0.8.The suspension was kept at room temperature in the dark for 2-3 hours.Healthy, approximately one-month-old *Nicotiana benthamiana* plants were selected, and the bacterial suspension was infiltrated into the abaxial side of tobacco leaves using a needleless syringe.After infiltration, plants were kept in darkness for 12 hours at 25°C, followed by 48-72 hours under light conditions.GFP fluorescence was observed and imaged using a confocal laser scanning microscope.

2.7 Virus-Induced Gene Silencing (VIGS) in *Z. armatum*

A conserved region of the *ZaTPS* sequence was selected for VIGS vector construction.The silencing vector pCAMBIA1301-35SN was linearized using the BamHI restriction site.Specific primers containing homologous arms to the vector ends were designed to amplify the target *ZaTPS* fragment.An intron fragment containing homologous sequences to the target was amplified using the intermediate vector pHANNIBAL as a template.The recombinant VIGS vector was constructed in the order: pCAMBIA1301-35SN - forward target fragment - intron - reverse target fragment - pCAMBIA1301-35SN, resulting in the *ZaTPS*-RNAi recombinant construct.The recombinant plasmid and the empty vector were introduced into A.tumefaciens GV3101.Bacterial suspensions were resuspended in MS medium to an OD600 of 0.6-0.8 and evenly sprayed onto the leaves of *Z. armatum* plants.

2.8 Transient Overexpression of *ZaTPS* in *Z. armatum*

For transient overexpression, the plant overexpression vector BG Plant-Express MCS was linearized at the KpnI site.Specific primers containing homologous arms to the linearized vector were designed to amplify the *ZaTPS* CDS.The *ZaTPS* fragment was ligated with the overexpression vector to generate the *ZaTPS*-OE recombinant construct.This construct was introduced into A.tumefaciens GV3101 using the same method described above.The bacterial suspension was resuspended in MS medium and evenly sprayed onto the leaves of *Z. armatum* plants.

2.9 Analysis of *ZaTPS* Expression Levels

Total RNA was extracted from all treated *Z. armatum* samples, reverse-transcribed into cDNA, and subjected to qRT-PCR analysis.The Actin gene served as an internal reference for relative gene expression quantification.Specific primers for *ZaTPS* were designed using NCBI Primer-BLAST, targeting amplicon sizes of 80-150 bp.

2.10 Measurement of Terpenoids in Zanthoxylum armatum

2.10.1 Extraction of Terpenoid Compounds

Healthy leaves from differently treated *Z. armatum* plants were collected, washed with distilled water, and dried.The leaves from each treatment group were separately ground into a fine powder and passed through a 40-mesh sieve.The powder was extracted with 75% ethanol in a conical flask.The ethanol was pre-filtered through a 0.22 μm membrane to remove impurities.The conical flask was placed in a constant temperature incubator shaker at 37°C and shaken at 200 rpm for 6 hours for extraction.After extraction, the mixture was filtered through qualitative filter paper to collect the filtrate.The filtrate was transferred to the evaporation flask of a rotary evaporator.The water bath temperature was set to 50°C and the vacuum to 0.06 MPa.Rotary evaporation was initiated and stopped when a viscous liquid appeared in the flask.The obtained crude extract was dissolved in chromatographic-grade methanol solution, and this solution served as the sample for subsequent analysis.

2.10.2 HPLC Detection

Linalool (Source Leaf, B20387-100mg) was used as the standard.It was dissolved in chromatographic-grade methanol and diluted to four concentration gradients: 100 μg/ml, 50 μg/ml, 25 μg/ml, and 10 μg/ml.The terpenoid content in the leaves of differently treated *Z. armatum* plants was measured using High-Performance Liquid Chromatography (HPLC).A 500 μl aliquot of the methanol solution from each group was transferred to a brown sample vial for injection.The mobile phase consisted of acetonitrile and deionized water.The flow rate was 1.0 ml/min, the column temperature was 30°C, the detection wavelength was set at 205 nm, and the injection volume was 10 μl.The HPLC parameters were as follows: mobile phase A was acetonitrile, and mobile phase B was deionized water.The following gradient elution program was employed (percentage of mobile phase A over time): isocratic elution at 10% for 10 minutes, linear gradient from 10% to 55% (10-15 min), isocratic elution at 50% (15-18 min), linear gradient from 50% back to 10% (18-20 min), and re-equilibration at 10% (20-25 min).

Using linear regression standard curve equation is obtained:

$$Y = k \cdot C + b$$

Among them: Y = peak area; C= Concentration (μg/ml); k= slope; b= Intercept.

The content of linalool in the sample is:

$$\text{Linalool content} = (C_{sample} \cdot V \cdot D)/m$$

Among them: Csample= linalool concentration in the machine solution (μg/ml); V= Sample volume (ml); D= Dilution factor; m= Sample weighing mass (g)

2.11 Expression Analysis of Genes Related to Terpene Synthesis

Plant terpene synthesis occurs via two pathways: the Methylerythritol Phosphate (MEP) pathway and the Mevalonate (MVA) pathway.To investigate changes in the terpene synthesis pathway in differently treated plants, the expression levels of six key genes were analyzed[16].These genes represent markers for the initiation of terpenoid synthesis or encode enzymes involved in pivotal steps: DXP (1-Deoxy-D-xylulose 5-phosphate, the starting metabolite), DXR (1-deoxy-D-xylulose-5-phosphate reductoisomerase, which catalyzes the conversion of DXP to MEP (2-C-Methyl-D-erythritol 4-phosphate), IPP (Isopentenyl pyrophosphate, the universal precursor for terpenoids), and the precursors for monoterpenes and sesquiterpenes, GPP (Geranyl pyrophosphate) and FPP (Farnesyl pyrophosphate).Corresponding sequences were screened from the *Z. armatum* transcriptome database.Specific qPCR primers were designed using NCBI Primer-BLAST.The Actin gene was used as the internal reference for normalizing gene expression.

2.12 Assay of Defense-related Enzyme Activities

Mature leaves from transiently expressed/treated plants and control plants were selected to determine the activities of defense-related enzymes: peroxidase (POD), catalase (CAT), superoxide dismutase (SOD), and the content of malondialdehyde (MDA).After treatments, healthy mature leaves were collected, washed with sterile water, dried, and ground into a fine powder using a grinder.Enzyme activities were measured using commercially available assay kits (Boxbio).Precisely 0.1 g of powder was homogenized in 1 ml of extraction buffer (1:10, w/v) on ice.The homogenate was centrifuged at 8000 rpm for 10 min at 4°C.The supernatant was collected and kept on

ice for immediate analysis.Absorbance was measured using a microplate reader, and enzyme activities were calculated according to the kit protocols.

2.13 Expression Pattern Analysis after Rust Infection and Pathogenicity Assay

To elucidate the expression pattern of the *ZaTPS* gene in response to rust infection, one-year-old plants of the susceptible 'Tengjiao' cultivar and the resistant 'Youkang' line were inoculated with *Coleosporium zanthoxyli* using a spore suspension method.Urediniospores, activated on water agar plates, were washed off with sterile water to prepare a spore suspension at a concentration of 10^6 spores/mL.The spore suspension was sprayed onto the leaves of 'Youkang' and 'Tengjiao' plants.Inoculated plants were maintained at 26°C and 90% relative humidity in a growth chamber with 24 hours of post-inoculation moisture retention.Control plants were sprayed with sterile water.Each treatment group consisted of three biological replicates.

From 0 to 20 days post-inoculation (dpi), leaf samples were collected at 5-day intervals using a five-point sampling method.Collected leaves were immediately frozen in liquid nitrogen and stored at -80°C for subsequent RNA extraction and cDNA synthesis.

Disease assessment was performed at 25 dpi.Disease incidence and disease index were calculated according to the criteria presented in Table 2.

Table 2 Disease Grading Criteria

Level	Representative value	Classification criteria
1	0	No summer (or winter) spore piles on the leaves
2	1	The number of spore colonies in summer (or winter) is 1 to 5 (accounting for less than 1/10 of the leaf area).
3	2	The number of spore colonies in summer (or winter) is 6 to 10 (accounting for about 1/10 to 1/3 of the leaf area)
4	3	The number of spore colonies in summer (or winter) is 11 to 15 (accounting for about 1/3 to 1/2 of the leaf area)
5	4	The number of spore colonies in summer (or winter) is greater than 15 (accounting for more than half of the leaf area)

- Incidence rate（%）$=\frac{\text{Number of disease strains}}{\text{Total volume according to inquiry}}\times 100$

$$\text{Disease index}=\frac{\sum(\text{Number of each disease grades}\times\text{Number of diseased seedlings})}{(\text{Total}\times\text{Highest level quantity})}\times 100$$

3. Results

3.1 Cloning and Bioinformatics Analysis of *ZaTPS*

3.1.1 Cloning of *ZaTPS*

Healthy young leaves from rust-resistant (R) and susceptible (S) *Z. armatum* plants were collected and immediately frozen in liquid nitrogen to prevent RNA degradation.Total RNA was extracted using the SteadyPure Plant RNA Extraction Kit.The integrity of the RNA was confirmed by agarose gel electrophoresis (Fig.1).First-strand cDNA was synthesized using total RNA as template.The amplified product of the target gene was analyzed by agarose gel electrophoresis (Fig.2).The product size was between 1000 and 1500 bp, consistent with the expected size of 1206 bp.The amplified product was sent to Tsingke Biotechnology Co., Ltd.(Beijing) for sequencing, ultimately obtaining the 1206 bp *ZaTPS* gene.

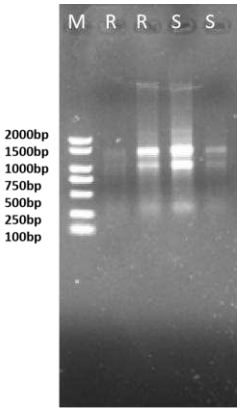

Figure 1 Electrophoresis diagram for total RNA integrity detection of *Z. armatum*

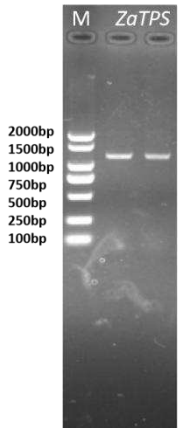

Figure 2 Electrophoresis diagram of *ZaTPS* amplification

3.1.2 Bioinformatics Analysis of *ZaTPS*

The coding sequence (CDS) of *ZaTPS* is 1206 bp long.Analysis of the deduced protein sequence revealed that the *ZaTPS* protein is 402 amino acids in length, with a theoretical isoelectric point (pI) of 5.38, indicating it is an acidic protein.The molecular weight is 46612.02 Da.The aliphatic index is 92.69, suggesting relatively high thermostability.The instability index is 57.33, classifying it as an unstable protein.The grand average of hydropathicity (GRAVY) is -0.122, classifying *ZaTPS* as a hydrophilic protein.Amino acid sequences of TPS genes from 10 different plant species were aligned using DNAMAN software.Subcellular localization prediction indicated cytoplasmic localization.Signal peptide and transmembrane domain analyses showed that *ZaTPS* lacks a signal peptide and transmembrane helices, classifying it as a non-secretory protein.Secondary structure prediction showed the protein is predominantly composed of alpha-helix (72.32%), followed by random coil (24.69%) and extended strand (2.99%).

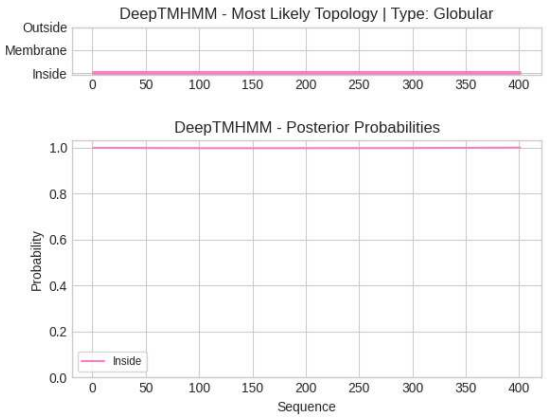

Figure 3 Prediction of *ZaTPS* Signal peptides

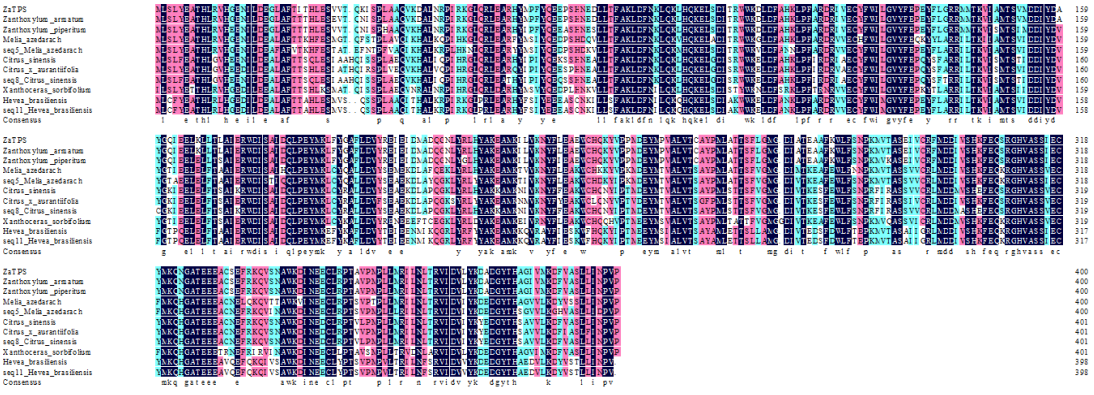

Figure 4 Homology comparison of amino acid sequences of *ZaTPS*

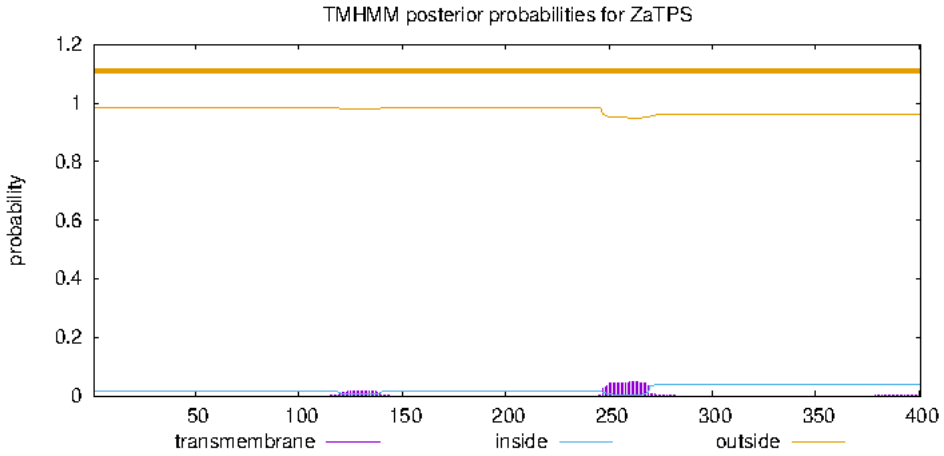

Figure 5 Prediction of *ZaTPS* transmembrane domains

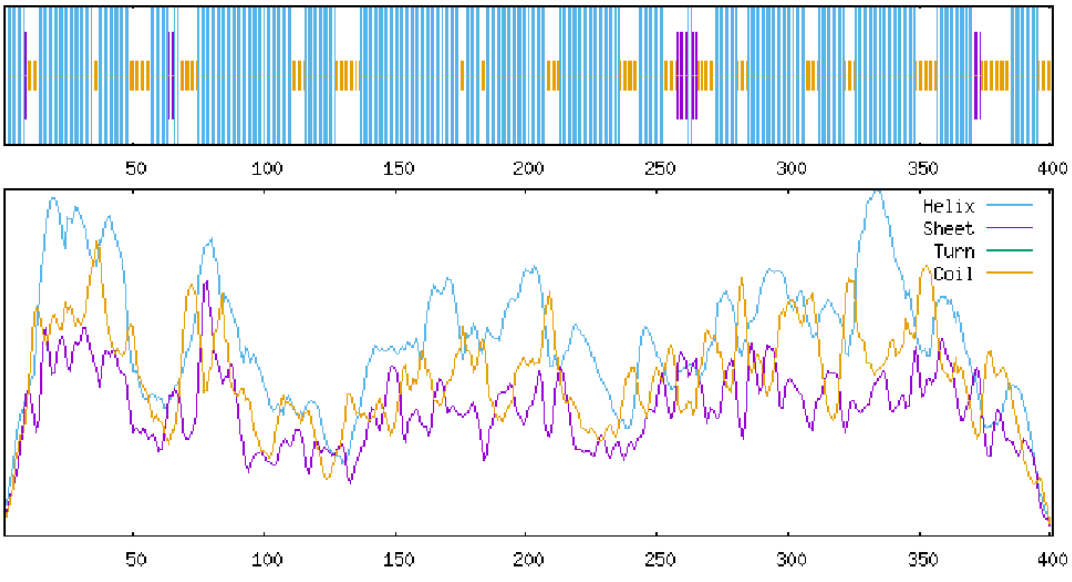

Figure 6 Prediction of *ZaTPS* Secondary Structure

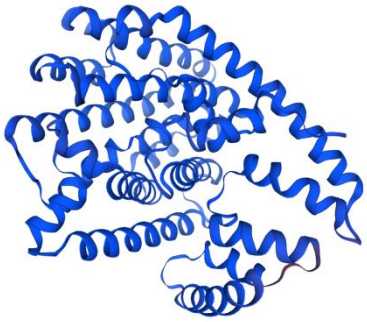

Figure 7 Prediction of the tertiary structure of *ZaTPS*

3.2 Expression Pattern Analysis

The expression patterns of *ZaTPS* in different tissues were analyzed.Results are shown in Fig.8.The expression level of *ZaTPS* was significantly higher in rust-resistant plants compared to susceptible plants.Within the same plant, the expression was highest in leaves, while relatively lower levels were detected in stems and roots.

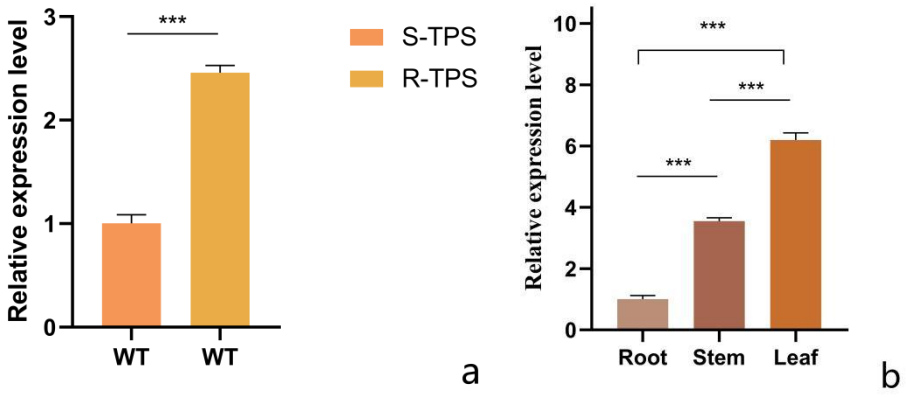

Figure 8 Expression levels of *ZaTPS* in anti-susceptibility plants and their roots, stems and leaves

Note: Figure a shows the expression level of *ZaTPS* in healthy plants; Figure b shows the expression levels of *ZaTPS* in the roots, stems and leaves of healthy anti-susceptibility plants.R (Resistance) : Healthy "Youkang" plant; S (Sensation) : Healthy "prickly ash" plant.*** indicates a significant difference at the P<0.001 level.

3.3 Subcellular Localization of *ZaTPS*

The *ZaTPS* fragment flanked by homologous arms for the GFP vector was amplified.The pCAMBIA1300-EGFP-MCS vector was linearized by single digestion using the KpnI site.The amplified *ZaTPS* fragment and the linearized vector were gel-purified.After confirmation, the *ZaTPS* fragment containing the vector homologous arms was ligated with the KpnI-digested linearized vector via homologous recombination.The recombinant product was transformed into E.coli DH5α.Single colonies were screened by colony PCR using vector-specific primers (1300YZ-F/R), and the product size was verified.

The obtained positive fusion plasmid (*ZaTPS*-GFP) was transformed into *Agrobacterium* tumefaciens GV3101 competent cells.Single colonies were again verified.The amplified *ZaTPS* fragment, including 16 bp homologous arms at both ends, had a theoretical length of 1238 bp.The electrophoretic band was located near 1000 bp.Colony PCR with vector-specific primers yielded a theoretical product of 1434 bp, with the band located between 1000-2000 bp.Sequencing of the PCR products confirmed correct insertion, indicating successful transformation into *Agrobacterium* for subsequent experiments.

The culture of *Agrobacterium* confirmed as positive was scaled up and infiltrated into the abaxial side of leaves of approximately one-month-old Nicotiana benthamiana plants.After infiltration, plants were incubated at 25°C in a growth chamber for 72 hours and then observed and imaged using a confocal laser scanning microscope.Results showed that GFP protein expressed from the pSuper1300-GFP positive control accumulated abundantly in cells, exhibiting a diffuse distribution pattern.Co-localization assays with nuclear and plasma membrane markers showed that the *ZaTPS*-GFP fusion protein signal did not overlap with the nuclear marker signal but partially overlapped with the plasma membrane marker signal, preliminarily suggesting cytoplasmic localization.

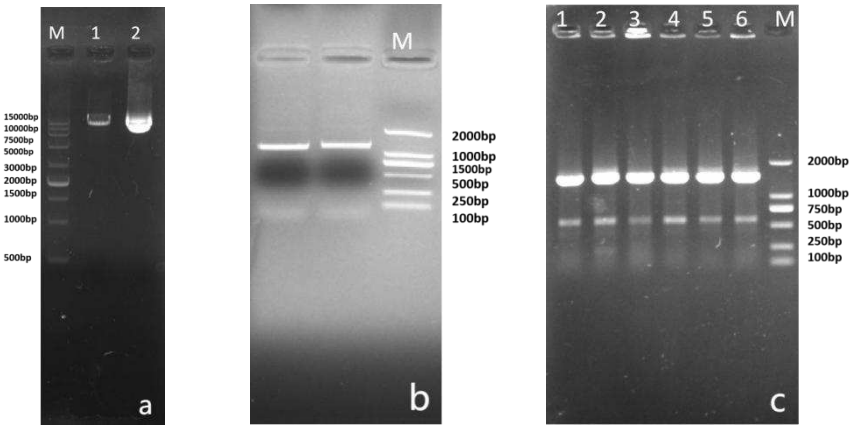

Figure 9 shows the electrophoresis of vector enzyme digestion, amplification of the homologous arm fragment of *ZaTPS* and verification of positive colonies

Note: Figure a shows the pCAMBIA1300-EGFP-MCS plasmid (Lane 2) and the linearized pCAMBIA1300-EGFP-MCS vector (Lane 1) after KpnI digestion, M: 15 K marker; Figure b shows the amplification of the *ZaTPS* gene with homologous arms, M: 2 K marker; Figure c shows the single colony verification of the fusion product *ZaTPS*-GFP.Lanes 1-6 are positive colonies, with M: 2 K marker.

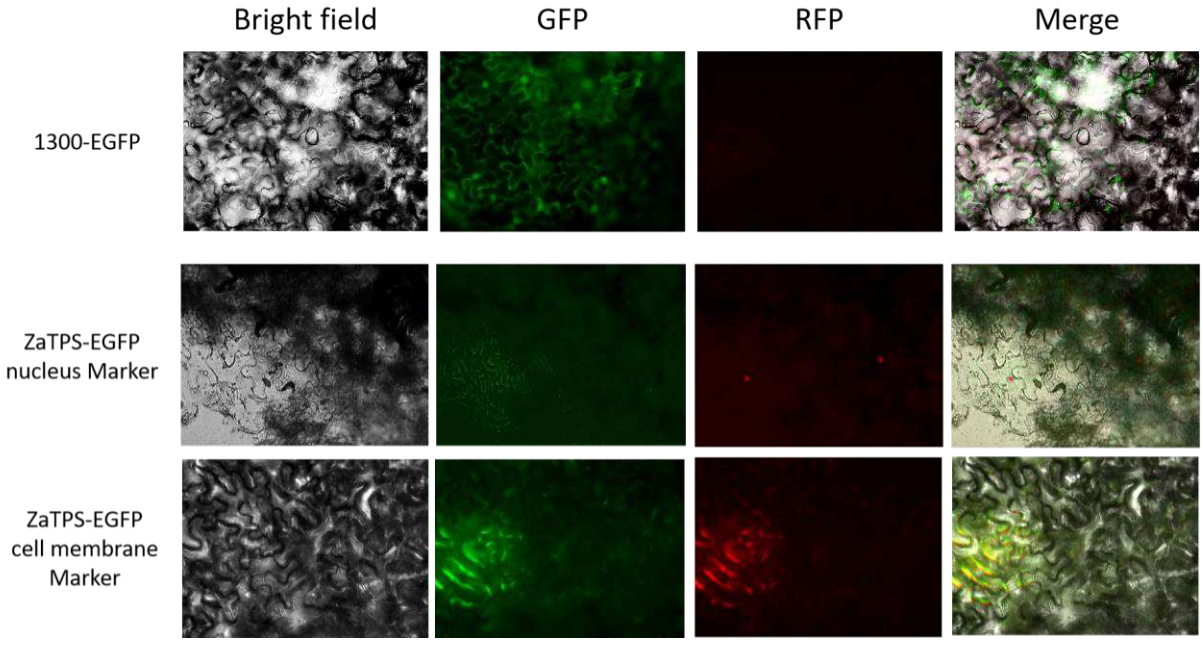

Figure 10 Subcellular localization of *ZaTPS*

3.4 Construction of the *ZaTPS*-RNAi Expression Vector

3.4.1 Amplification of Interference and Intron Fragments

The forward *ZaTPS* fragment was designed with a 15 bp vector homologous sequence at the 5' end and an 8 bp intron homologous sequence at the 3' end, resulting

in a theoretical length of 426 bp.The reverse *ZaTPS* fragment had a 14 bp intron homologous sequence at the 5' end and a 21 bp vector homologous sequence at the 3' end, resulting in a theoretical length of 438 bp.The PDK intron region (769 bp) from the intermediate vector pHANNIBAL was amplified with 13 bp and 12 bp homologous arms complementary to the ends of the forward and reverse fragments at its 5' and 3' ends, respectively, resulting in an "M-intron" fragment with a theoretical length of 794 bp.Agarose gel electrophoresis showed that lanes 1 and 2 (forward fragments) and lanes 7 and 8 (reverse fragments) displayed bands near 500 bp.Lanes 3-6 (intron fragment) displayed bands near 750 bp.All bands were of the correct size with sharp edges.Sequencing confirmed their accuracy, allowing their use for vector construction.

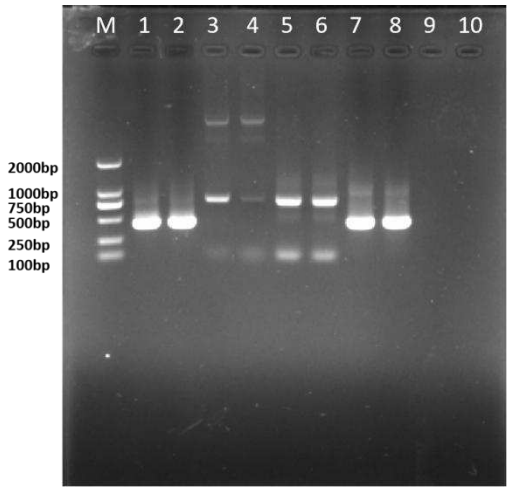

Figure 11 Electrophoresis images of forward, intron and reverse fragment amplification of *ZaTPS*

Note: 2 K marker; Lanes 1 and 2 are the forward interference fragments of *ZaTPS*, lanes 3 to 6 are intron fragments, and lanes 7 and 8 are the reverse interference fragments of *ZaTPS*

3.4.2 Linearization of the pCAMBIA1301-35SN Vector

The circular pCAMBIA1301-35SN plasmid (13,044 bp) appears as a wide, diffuse band on a gel.After digestion with BamHI, a single, sharp band was observed, indicating complete digestion and successful linearization.The linearized vector was purified and stored.

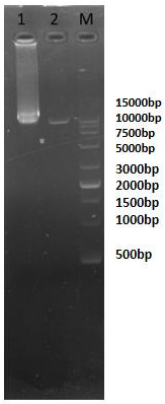

Figure 12 Linearization of pCAMBIA1301-35SN

Note: M: 15 K marker; 1: pCAMBIA1301-35SN plasmid 2: Linearized vector processed by BamHI single-enzyme digestion.

3.4.3 Homologous Recombination

The forward *ZaTPS* fragment, intron fragment, reverse *ZaTPS* fragment, and the linearized pCAMBIA1301-35SN vector were assembled via homologous recombination.The recombinant product was transformed into E.coli.Due to potential hairpin structure formation during PCR amplification because of the identical sequences in the forward and reverse fragments, bidirectional verification using primers designed at the vector and intron junctions was necessary to confirm successful assembly.Single colonies were subjected to PCR using primer pairs 01-F/Ph-R (expected product ~608 bp for *ZaTPS* segment) and Ph-F/01-R (expected product ~484 bp).Colonies positive for both primer pairs were considered positive (Fig.13 shows colonies 1-4 were positive).Sequencing confirmed the successful construction of the *ZaTPS*-RNAi silencing vector.Positive colonies were cultured for plasmid extraction, and glycerol stocks were prepared and stored at -80°C.The confirmed *ZaTPS*-RNAi recombinant plasmid was transformed into A.tumefaciens for subsequent experiments.

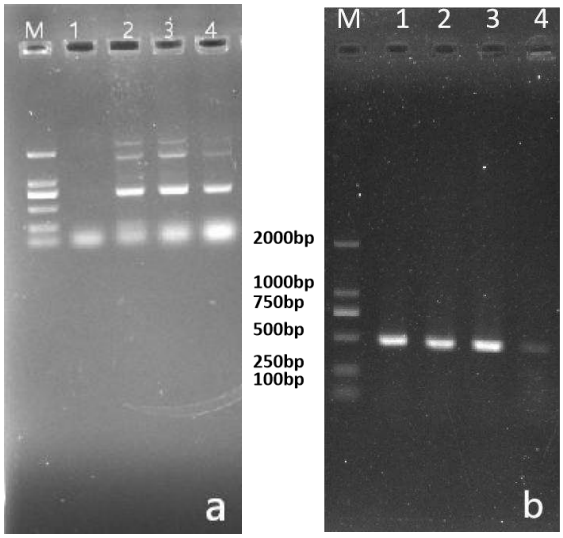

Figure 13 Verification of positive colonies

Note: Figure a shows the positive clones of *ZaTPS*-RNAi detected by 01-F/Ph-R primers; Figure b shows the positive clone detection of *ZaTPS*-RNAi detected by Ph-F/01-R primers.

3.5 Construction of the *ZaTPS* over-expression Vector

3.5.1 Fragment Amplification

The full-length *ZaTPS* sequence was amplified with a 13 bp homologous arm at the 5' end and a 20 bp homologous arm at the 3' end.The theoretical length of the *ZaTPS*-OE fragment was 1239 bp.Agarose gel electrophoresis showed a band of the correct size with sharp edges.Sequencing confirmed its accuracy.The fragment was gel-purified for subsequent steps.

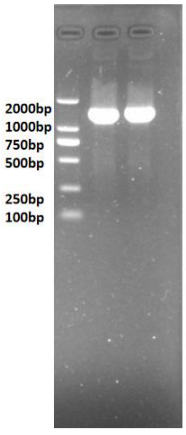

Figure 14 Amplification of *ZaTPS* fragments with homologous arms

3.5.2 Linearization of BG Plant-Express MCS

The circular BG Plant-Express MCS plasmid (9676 bp) appears as a very wide, diffuse band on a gel.Digestion with KpnI yielded a single, sharp band, indicating complete linearization.The linearized vector was purified for subsequent experiments.

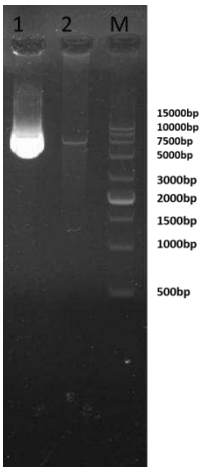

Figure 15 BG Plant-Express MCS linearization

Note: M: 15 K marker; 1: BG Plant-Express MCS plasmid; 2-5: Expression vectors single-digested by KpnI endonuclease.

3.5.3 Homologous Recombination

The gel-purified *ZaTPS* fragment containing the vector homologous arms and the gel-purified linearized BG Plant-Express MCS vector were assembled via homologous recombination.The product was transformed into E.coli.Single colonies were screened by colony PCR using primers KpNIOE-F/R, yielding a theoretical product of 1449 bp.Agarose gel electrophoresis (Fig.3-15) showed bright bands of the correct size for lanes 1, 3, and 4.Sequencing confirmed no errors, indicating the successful construction of the *ZaTPS* overexpression vector (*ZaTPS*-OE).Positive colonies were cultured for plasmid extraction.Glycerol stocks of E.coli harboring *ZaTPS*-OE were prepared and stored at -80°C.The extracted *ZaTPS*-OE recombinant plasmid was transformed into A.tumefaciens for the next experiments.

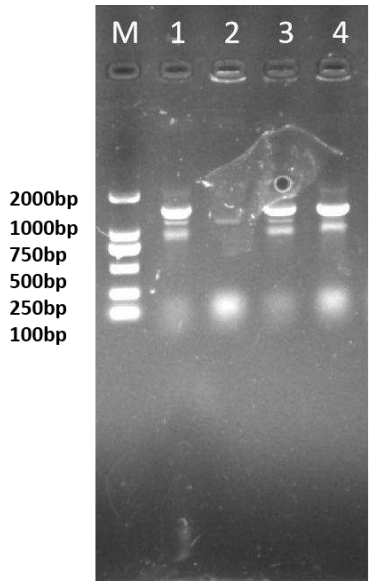

Figure 16 Colony verification of the *ZaTPS*-OE recombinant plasmid

3.6 Generation of Transiently Transformed Plants

3.6.1 Validation of Positive Plants

Twenty days after agroinfiltration, three plants each for *ZaTPS*-RNAi, *ZaTPS*-OE, pCAMBIA1301-35SN empty vector control, and BG Plant-Express MCS empty vector control were obtained.Plants treated with sterile water served as negative controls.PCR amplification using primers for the Kanamycin resistance gene was performed to identify and screen positive plants for overexpression and silencing constructs.The amplified fragment sizes were as expected.Results confirmed successful transformation of *Z. armatum* leaves with *Agrobacterium* carrying *ZaTPS*-RNAi and *ZaTPS*-OE, allowing further functional validation.

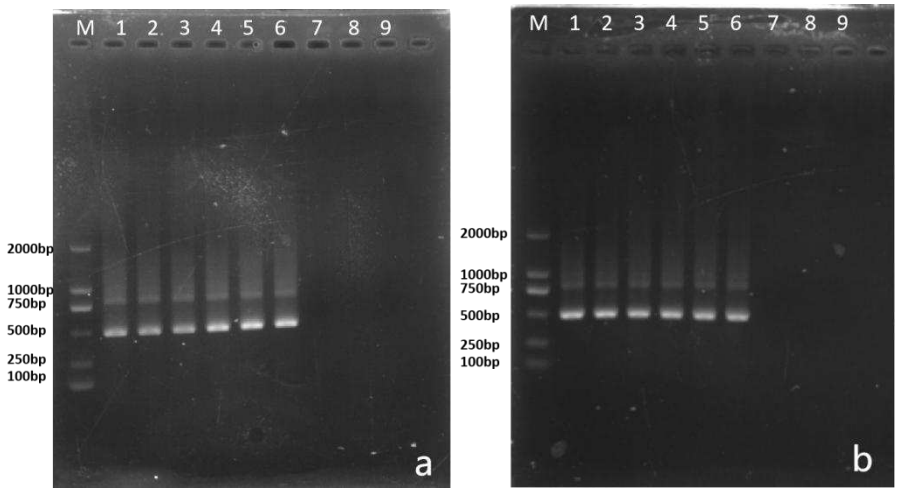

Figure 17 PCR detection of positive transformed strains

Note: Figure a shows the *ZaTPS*-RNAi detection, and Figure b shows the *ZaTPS*-OE detection.All M are 2-K markers.1-3 represent positive controls, 4-6 represent positive transformed strains, and 7-9 represent negative controls.

3.6.2 Validation of Gene Expression Levels

To verify whether transient transformation achieved gene silencing or overexpression, qRT-PCR was performed on transiently transformed plants, using wild-type plants as control.Results showed that the transcript level of *ZaTPS* in leaves of silencing transformants was significantly lower than in wild-type, while it was significantly higher in overexpression transformants.This indicates that the in vitro synthesized recombinant vectors effectively mediated gene silencing and overexpression of the target gene.

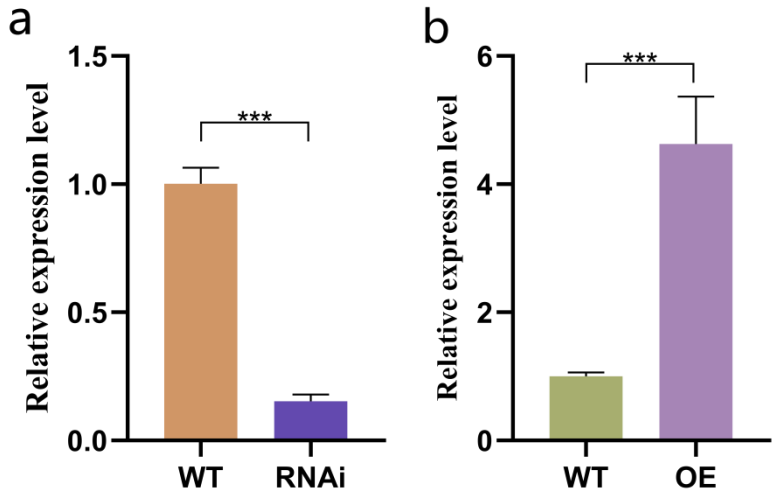

Figure 18 Analysis of the expression level of *ZaTPS* in transient transformation strains

Note: Figure a shows the analysis of the expression level of the *ZaTPS* gene in the transient silenced transformation strain; Figure b shows the analysis of the expression level of the *ZaTPS* gene in the transient overexpression transformation strain.*** indicates a significant difference at the $p<0.001$ level.

3.7 Determination of Terpene Content

3.7.1 Effect of Linalool on Rust Spore Germination

The germination rate of rust spores was observed microscopically on water agar plates six hours after applying spore suspensions.In the control group, the spore germination rate reached 96%, while on water agar plates supplemented with linalool, the germination rate was 0%.This indicates that linalool, as a terpenoid compound, can effectively inhibit rust spore germination.

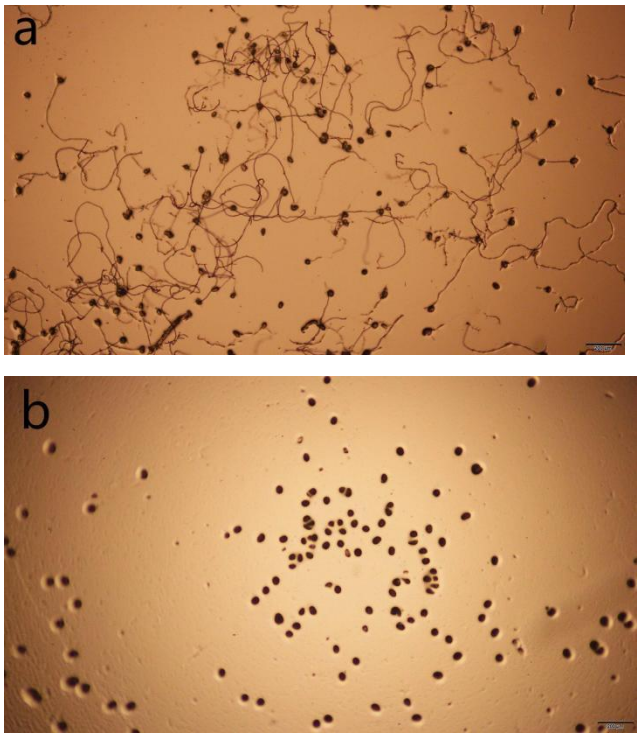

Figure 19 Inhibitory effect of linalool on the germination of uredospores

Note: Figure a shows the normal germination of uredospores; Figure b shows the germination status of uredospores when 100 μg/ml linalool is added.

3.7.2 HPLC Measurement of Linalool Content in Differently Treated Plants

After measuring samples of different standard concentrations and different treatments, a regression analysis was performed using concentration (μg/mL) as the independent variable (X) and peak area integration value as the dependent variable (Y) to create a standard curve (Fig.20).The regression equation was Y = 180596X + 2E+06, with a correlation coefficient R^2 = 0.9697, indicating a good linear relationship between linalool peak area and injection concentration within the 20–100 μg range.The chromatogram of the standard (Fig.21) showed a peak at 14.467 min.The linalool content in different treatment groups was calculated using the formula and is presented in Table 3.The results show that compared to the control plants, transient expression of *ZaTPS* significantly affected linalool content.It can be concluded that *ZaTPS* is involved in the rust resistance process of *Z. armatum* by altering its linalool content.

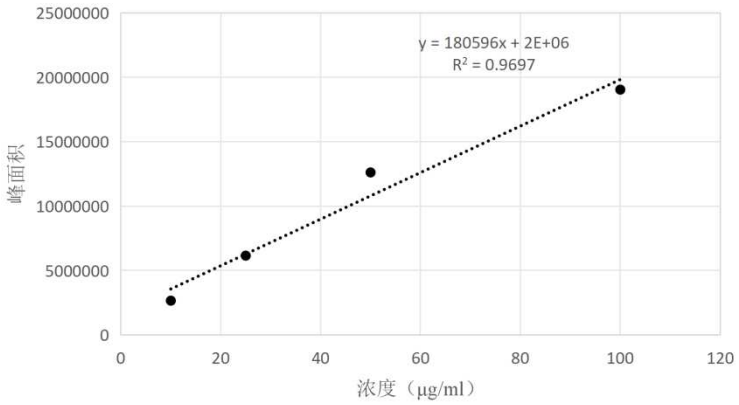

Fig 20 Linear Relationship of Linalool

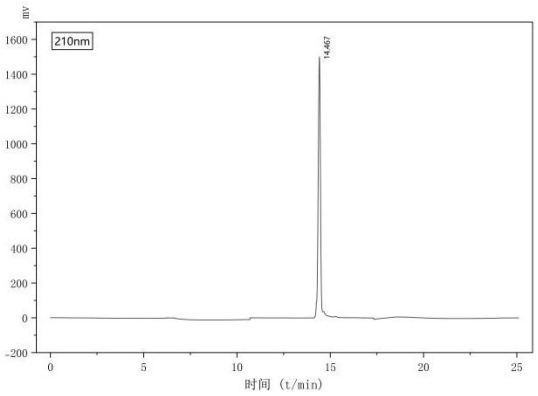

Figure 21 HPLC Chromatogram of Linalool

Table 3 Content of Linalool in Different Treated Plants (n = 3)

Plants	Linalool conten（mg/g）	RSD（%）
WT	8.12[b]	1.92
TPS-OE	9.61[a]	3.85
TPS-RNAi	6.14[c]	2.46

3.8 Analysis of Related Gene Expression in *ZaTPS* Transiently Expressed Plants

To investigate the effect of *ZaTPS* overexpression and silencing on genes related to terpenoid biosynthesis, six key genes from the plant MEP terpene synthesis pathway were selected for expression analysis in differently treated plants.These genes included: DXP (1-Deoxy-D-xylulose 5-phosphate, the marker metabolite for the initiation of terpenoid synthesis), DXR (1-deoxy-D-xylulose-5-phosphate reductoisomerase, which catalyzes the conversion of DXP to MEP (2-C-Methyl-D-erythritol 4-phosphate), IPP (Isopentenyl pyrophosphate, the universal precursor for terpenoids), and the precursors for monoterpenes and sesquiterpenes,

GPP (Geranyl pyrophosphate) and FPP (Farnesyl pyrophosphate).Specific qPCR primers were designed for each gene using NCBI Primer-BLAST to investigate changes in the terpene synthesis pathway in differently treated plants.

Analysis of expression levels of these related genes in transiently overexpressed and silenced transformants showed that the expression of some related genes was significantly upregulated in overexpression transformants, while it was significantly downregulated in silencing transformants.

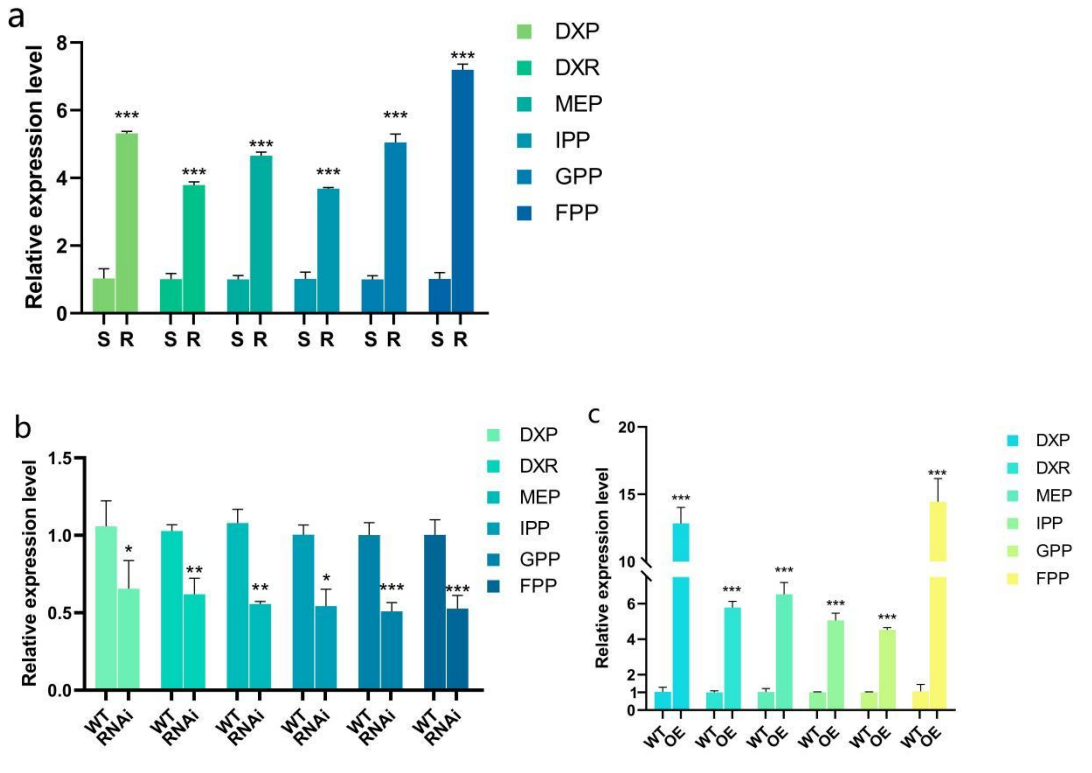

Figure 22 Analysis of the expression levels of terpene synthesis-related genes in wild anti-susceptibility strains and transient transformation strains

Note: Figure a shows the analysis of the expression levels of related genes in the anti-R (S) strain; Figure b shows the analysis of the expression levels of related genes in the transient silenced transformation strain.Figure c shows the analysis of the expression levels of related genes in the transient overexpression transformation strain.*, * * and * * *, respectively, $p < 0.05$, $p < 0.01$, $p < 0.001$ significant level.

3.9 Measurement of Defense-related Enzyme Activities

The activities of catalase (CAT), superoxide dismutase (SOD), peroxidase (POD), and the content of malondialdehyde (MDA) were measured in treated plants.CAT primarily catalyzes the decomposition of hydrogen peroxide (H_2O_2), protecting cells from free radical damage and playing a crucial role in the reactive

oxygen species (ROS) scavenging system.SOD is a metalloenzyme that catalyzes the dismutation of superoxide anions into H_2O_2 and O_2, playing a vital role in the biological antioxidant system.POD catalyzes various reactions involving H_2O_2 during cellular redox metabolism and participates in clearing ROS produced during pathogen infection to prevent cellular damage.MDA is a final product of lipid peroxidation, possessing cytotoxicity and capable of cross-linking macromolecules like proteins and nucleic acids.Measuring MDA content reflects the rate and intensity of lipid peroxidation and indirectly indicates the degree of oxidative damage in tissues.

Measurement of CAT activity revealed significant differences between *ZaTPS* transiently silenced plants, overexpression plants, and control plants.The activities of SOD and POD followed a trend consistent with CAT activity, showing significant differences between differently treated plants and controls.MDA activity, reflecting lipid peroxidation, showed an opposite trend compared to CAT, SOD, and POD activities.MDA levels were significantly higher in silenced plants than in overexpression plants.These results indicate that silencing and overexpression of *ZaTPS* differentially alter the activities of defense-related enzymes.

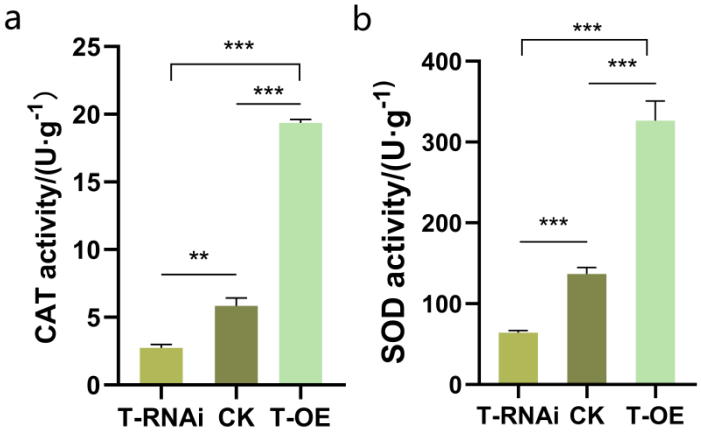

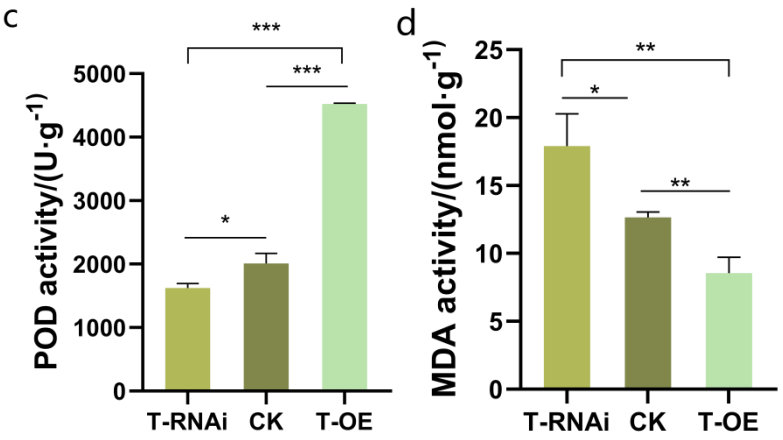

Figure 23 Partial defense enzyme activity of the treated strain

Note: Figure a shows the CAT enzyme activities of different treatment strains; Figure b shows the SOD enzyme activities of different treatment strains; Figure c shows the enzymatic activities of POD in different treatment strains.Figure d shows the MDA enzyme activities of different treatment strains.T-RNAi: *ZaTPS* silenced strain; T-OE: Overexpressing strain of *ZaTPS*; CK: controlled plant *, * * and * * *, respectively, $p < 0.05$, $p < 0.01$, $p < 0.001$ significant level.

3.10 Inoculation of Transformed Plants with Rust Spores

3.10.1 Rust Resistance Levels in Transformed Plants

Fresh *C.zanthoxyli* spores were collected and used to prepare a suspension for inoculating different transiently transformed plants and controls.Disease symptoms observed 18 days post-inoculation (dpi) are shown in Fig.25.The control leaves showed distinct orange-yellow pustules covering approximately half of the abaxial leaf surface.The silencing treatment group exhibited the most severe symptoms, with *ZaTPS*-silenced plants showing stronger symptoms than control plants.In contrast, *ZaTPS*-overexpressing plants developed chlorotic spots on the abaxial surface, with a disease severity lower than the control.

Statistical analysis showed that compared to the control disease incidence of 43.69%, *ZaTPS*-silenced plants had the highest incidence (57.5%), while overexpression plants had the lowest (29.18%).The disease index was highest for *ZaTPS*-silenced plants (40.83) and lowest for overexpression plants (13.57).Both values were significantly different from the control disease index (31.39).In summary, these results indicate that the *ZaTPS* gene, as a disease resistance gene, participates in the defense process of *Z. armatum* against rust.

Figure 24 Plant diagrams of different treatments

Note: Figure A shows the silent treatment strain of *ZaTPS*; Figure B shows the strain treated with *ZaTPS* overexpression; Figure C shows the control plant

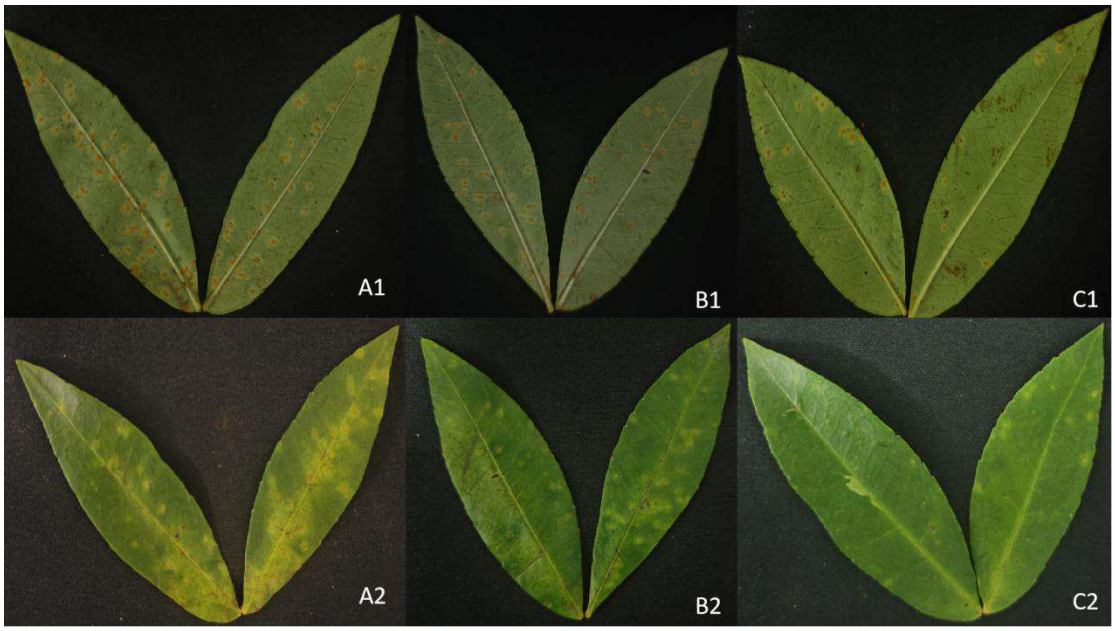

Figure 25 shows the symptoms of the plants used in the experiment after inoculation

Note: A1 and A2 are the leaf backs and leaf surfaces of the *ZaTPS* silencing treatment plants, respectively.B1 and B2 were respectively compared with the back and surface of the leaves of the plants.C1 and C2 are respectively the leaf dorsal and surface of the *ZaTPS* overexpression treated plants

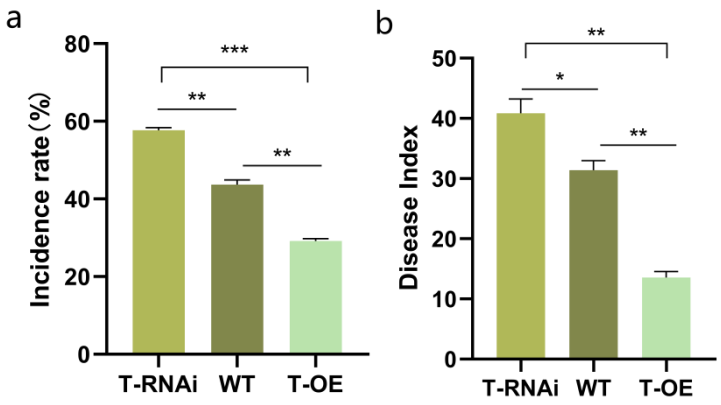

Figure 26 shows the incidence rate and disease index of transient expressed plants

Note: Figure a shows the incidence rate of the treated plants; Figure b for processing plant disease index of *, * * and * * *, respectively, $p < 0.05$, $p < 0.01$, $p < 0.001$ significant level.

3.10.2 Changes in Defense Enzyme Activities after Rust Inoculation in Transformed Plants

Leaves from different treated plants were collected 1 dpi to measure CAT, SOD, POD, and MDA activities, and compared with activities from non-inoculated plants of the same treatments.One day after rust inoculation, both *ZaTPS* overexpression and silencing plants showed a slight increase in enzyme activities compared to their non-inoculated counterparts.Among inoculated plants, *ZaTPS*-overexpressing plants showed the highest CAT activity (26.3 U/g), while *ZaTPS*-silenced plants showed the lowest (3.9 U/g).SOD activity also increased significantly in all plants 1 dpi compared to non-inoculated plants.*ZaTPS*-overexpressing plants had the highest SOD activity (593.7 U/g), while silenced plants had the lowest (192.6 U/g).POD activity followed a similar pattern, with *ZaTPS*-overexpressing plants showing the highest activity (7258 U/g) and silenced plants the lowest (1832 U/g) 1 dpi.MDA content, reflecting lipid peroxidation damage, decreased in all treated plants 1 dpi compared to non-inoculated plants.Among inoculated plants, *ZaTPS*-overexpressing plants had the lowest MDA content (2.0 nmol/g), while silenced plants had the highest (4.3 nmol/g).These results indicate that the activities of CAT, SOD, POD, and MDA in *Z. armatum* plants change significantly one day after rust inoculation, and these activities differ among plants subjected to *ZaTPS* silencing or overexpression, suggesting the involvement of *ZaTPS* in rust resistance.

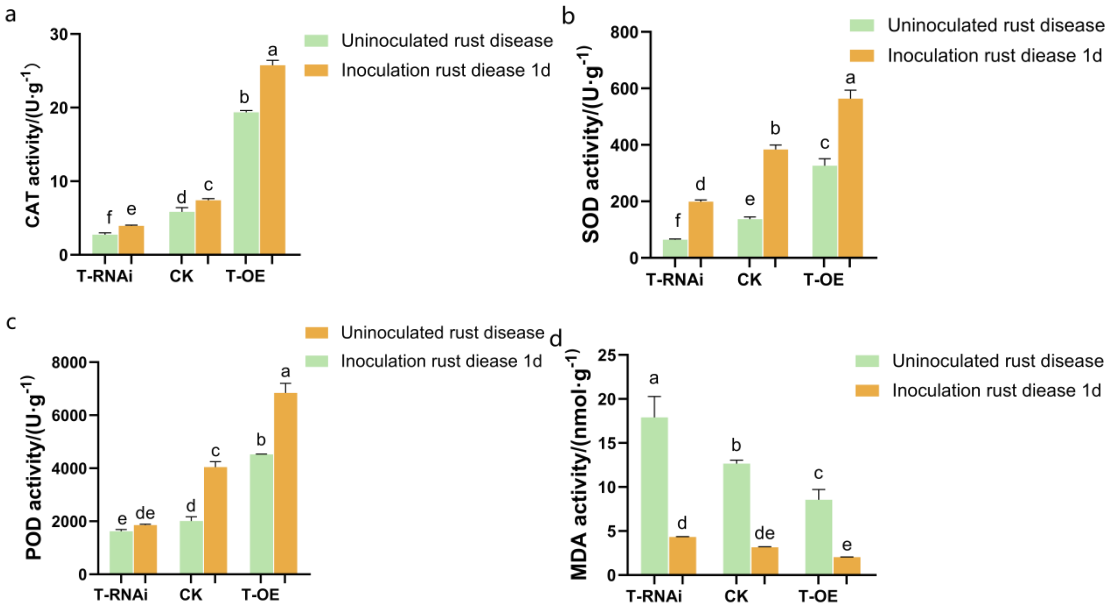

Figure 27 shows the transient expression of defense enzyme activities in plants and uninoculated plants one day after inoculation with rust spores

Note: Figure a shows the CAT enzyme activities of different treatment strains without rust spore inoculation and 1 day after rust spore inoculation.Figure b shows the SOD enzyme activities of different treatment strains without rust spore inoculation and 1 day after rust spore inoculation.Figure c shows the POD enzyme activities of different treatment strains without rust spore inoculation and 1 day after rust spore inoculation.Figure d shows the MDA enzyme activities of different treated strains without rust spore inoculation and 1 day after rust spore inoculation.T-RNAi: *ZaTPS* silenced strain; T-OE: Overexpressing strain of *ZaTPS*; CK: controlled plant after inoculated with different lowercase letters mark said different at 0.05 level between treatment group had significant difference (LSD test)

3.10.3 Changes in *ZaTPS* Expression after Rust Inoculation in Transformed Plants

To investigate the expression pattern of *ZaTPS* during rust resistance, leaves from susceptible plants were collected at 5-day intervals after spore inoculation.RNA was extracted, checked for integrity, reverse-transcribed to cDNA, and used for *ZaTPS* expression analysis at different time points.Results (Fig.28) showed that *ZaTPS* expression followed a trend of initial increase followed by a decrease over time post-inoculation, peaking at 15 dpi.This indicates that *ZaTPS* gene expression is associated with rust resistance in *Z. armatum*.

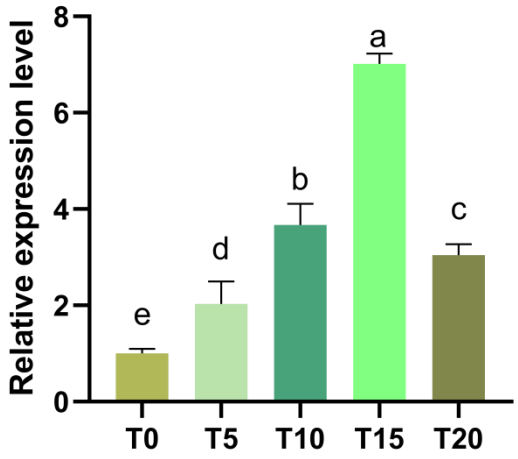

Figure 28 Analysis of *ZaTPS* expression levels at different times after inoculation with rust spores

4. Discussion

This study preliminarily reveals the crucial role of the *ZaTPS* gene in the response of *Zanthoxylum armatum* to rust disease stress. The results demonstrate that the expression level of this gene is significantly higher in resistant cultivars than in susceptible ones and exhibits leaf-specific high expression, closely aligning with the primary infection sites of the pathogen. Currently, the application of gene overexpression and silencing to study gene functions is widespread across various fields, including plants[29], animals[30], and medicine[31]. In this experiment, the successful construction of *ZaTPS* overexpression and silencing plants via *Agrobacterium*-mediated transient transformation confirmed the gene's functional manipulability.

We found that overexpression of *ZaTPS* significantly increased the content of the monoterpenoid linalool in *Z. armatum* leaves. In vitro antifungal assays further confirmed that linalool strongly inhibits the germination of *Coleosporium zanthoxyli* urediniospores. This aligns with findings in grapevine regarding the inhibition of Botrytis cinerea by monoterpenoids[32], revealing a direct biochemical mechanism for *ZaTPS*-mediated resistance: constructing a chemical barrier during the initial stages of pathogen infection by catalyzing the synthesis of antimicrobial terpenoid compounds. Concurrently, *ZaTPS* overexpression significantly upregulated the expression levels

of several key genes in the MEP pathway of terpenoid biosynthesis (e.g., DXP, DXR, IPP), indicating its positive regulatory role over the entire terpenoid metabolic pathway.

The reactive oxygen species (ROS) burst is an early event in the plant's response to pathogen infection, but excessive ROS can cause oxidative damage[33-34]. At the physiological defense level, *ZaTPS* expression significantly influenced the plant's antioxidant system. Following rust inoculation, the activities of catalase (CAT), superoxide dismutase (SOD), and peroxidase (POD) were significantly enhanced in overexpression plants, while the content of the lipid peroxidation product malondialdehyde (MDA) was significantly reduced[35-38]. By improving the efficiency of the antioxidant enzyme system, *ZaTPS* helps plants more effectively scavenge ROS and maintain membrane integrity, thereby mitigating oxidative stress damage[39]. This mechanism of enhancing disease resistance by priming the basal defense state is consistent with reports by Zhang et al.[40] on the involvement of terpenoids in systemic acquired resistance. Notably, the expression dynamics of *ZaTPS* are closely related to disease progression. During rust infection, *ZaTPS* expression showed an initial increase followed by a decrease, peaking at 15 days post-inoculation. This indicates that its induced expression is an important component of the active defense response in *Z. armatum*. This temporal expression pattern of *ZaTPS*, similar to trends reported in numerous related studies[41-43], further supports its functional role in disease resistance.

Although *ZaTPS* overexpression significantly increased linalool content and enhanced disease resistance, the causal relationship between expression changes of other genes in the terpenoid biosynthesis pathway and the final disease resistance phenotype is not fully elucidated. Furthermore, whether *ZaTPS* indirectly affects the defense response by regulating defense hormone signaling pathways such as jasmonic acid or salicylic acid remains to be investigated. Jasmonate-induced bHLH transcription factors have been shown to regulate terpene synthesis and influence resistance to insects and pathogens[44], suggesting that *ZaTPS* may reside within a more complex regulatory network.

Based on the silencing and overexpression of the *ZaTPS* gene and subsequent inoculation, this study found that the expression levels of some genes in the terpenoid synthesis pathway in treated *Z. armatum* plants changed differently, and corresponding changes also occurred upon rust spore infection. Simultaneously, the activities of the measured defense enzymes showed varying degrees of change. These results preliminarily demonstrate that *ZaTPS* plays a multi-layered defensive role in the rust resistance of *Z. armatum*: providing direct chemical defense through the synthesis of antimicrobial terpenoids and indirect physiological defense by enhancing the antioxidant system. These findings not only provide new insights into the molecular mechanisms of rust resistance in *Zanthoxylum* but also offer a potential target gene for breeding disease-resistant cultivars through genetic engineering. Future research should focus on deciphering the upstream regulatory mechanisms of *ZaTPS* and its interactions with other defense signaling pathways to comprehensively elucidate its functional positioning within the plant immune network.

5 Conclusion

This study confirms that the terpene synthase gene *ZaTPS* plays an indispensable positive regulatory role in the rust resistance of *Zanthoxylum armatum*. Utilizing transient overexpression and silencing techniques, it was demonstrated that high-efficiency expression of *ZaTPS* significantly enhances the synthesis and accumulation of the key monoterpenoid component linalool in leaves, directly inhibits the germination of *Coleosporium zanthoxyli* spores, and thereby establishes an effective chemical barrier during the early stages of infection. Concurrently, *ZaTPS* systematically reinforces terpenoid biosynthesis by upregulating the expression of key genes in the MEP pathway. At the physiological defense level, *ZaTPS* expression effectively enhances the plant's antioxidant defense capacity, as evidenced by significantly increased activities of key enzymes, including CAT, SOD, and POD, along with reduced membrane lipid peroxidation damage. Collectively, these functions confer a substantially lower disease incidence and severity index in overexpression plants. The specific temporal expression pattern of *ZaTPS* during rust

infection further corroborates its functional role as an integral component of the active defense response. Through a multidimensional synergistic mechanism encompassing chemical defense, metabolic regulation, and physiological protection, *ZaTPS* serves as a central hub in enabling *Z. armatum* to withstand rust stress. The findings of this research provide critical genetic resources and a theoretical foundation for further elucidating the molecular mechanisms of disease resistance in *Zanthoxylum* and for advancing targeted breeding strategies.

Statements

Data availability

The gene sequences used in this study are available at the following website: https://figshare.com/articles/dataset/The_chromosome-level_genome_assembly_of_Sichuan_pepper/14400884/1, number as Zardc21150.t1.

Abbreviations

TPS:*Terpene Synthases*

DXP:1-Deoxy-D-xylulose 5-phosphate

DXR:1-deoxy-D-xylulose-5-phosphate reducing isomerase

MEP:2-C-Methyl-D-erythritol 4-phosphate

IPP:Isopentenyl pyrophosphate

GPP:Geranyl pyrophosphate synthetase

FPP:Farnesyl pyrophosphate

AS:Acetosyringone

MES:2-Morpholinoethanesulphonic acid

PI:isoelectric point

CAT:catalase

SOD:superoxide dismutase

POD:peroxidase

MDA:malondialdehyde

Conflict of interest

The authors declare that the research was conducted in the absence of any commercial or financial relationships that could be construed as a potential conflict of interest.

Funding

The author(s) declare that financial support was received for the research and/or publication of this article. This research was funded by the General Project of Sichuan Provincial Department of Science and Technology (24NSFSC0799).

Author contributions

Yingming Lai: Conceptualization, Formal Analysis, Methodology, Writing – original draft, Writing – review & editing. Xingyu Liu: Formal Analysis, Methodology, Writing – review & editing. Li Zhao: Formal Analysis, Methodology, Writing – review & editing. Tianhui Zhu: Conceptualization, Supervision, Writing – review & editing. Shuying Li: Methodology, Writing – review & editing. Shujiang Li: Methodology, Resources, Writing – review & editing. Meng Ye: Resources, Writing – review & editing. Chunlin Yang: Methodology, Software, Writing – review & editing. Yujue Zhou: Formal Analysis, Methodology, Writing – review & editing. Shan Han: Conceptualization, Investigation, Methodology, Writing – original draft, Writing – review & editing.

Acknowledgements

Not applicable.

References

[1] Lianwen S, Shengqun C, Mei L, et al. Comparative analysis of codon usage bias in chloroplast genomes of ten medicinal species of Rutaceae. BMC Plant Biology, 2024, 24(1):424-424.

[2] Yang H, Lu T, Jingwei S, et al. Genetic structure of cultivated *Zanthoxylum* species investigated with SSR markers. Tree Genetics & Genomes, 2018, 14(6):1-9.

[3] Xue C, Lu T, Jieyun T, et al. Extensive Sampling Provides New Insights into Phylogenetic Relationships between Wild and Domesticated *Zanthoxylum* Species in China. Horticulturae, 2022, 8(5):440-440.

[4] Mengji C, Song Z, Ruiling L, et al. Spatial Virome Analysis of *Zanthoxylum armatum* Trees Affected With the Flower Yellowing Disease . Frontiers in Microbiology, 2021,

12:702210.

[5] Jingzhi Y, Chunxu C, Xianhui Y, et al. Didymella Segeticola;is a new pathogen causing leaf spot disease on *Zanthoxylum bungeanum*. New Zealand Journal of Crop and Horticultural Science, 2023, 51(4):694-703.

[6] Xu Z, Olmi M, Guglielmino A, et al. Description of a New Species of *Aphelopus Dalman* from China (Hymenoptera: Chrysidoidea: Dryinidae). Journal of the Kansas Entomological Society, 2011, 84(4):298-303.

[7] Yun R, Jiamin L, Liangping H, et al.Effect of Salicylic Acid Treatment on Disease Resistance to *Coleosporium zanthoxyli* in Chinese pepper (*Zanthoxylum armatum*)..Plant disease,2023,108(4):960-970.

[8] Li P, Cao Z, Wu Z, et al. The Effect and Action Mechanisms of Oligochitosan on Control of Stem Dry Rot of *Zanthoxylum bungeanum*. International Journal of Molecular Sciences, 2016, 17(7):1044- 1044.

[9] Gardner A K, Love B, Basler B P, et al. Genome-wide association analysis identifies seven loci conferring resistance to multiple wheat foliar diseases, including brown and yellow rust resistance originating from Aegilops ventricosa. Theoretical and Applied Genetics, 2025, 138(6):133-133.

[10] Xu X, Hu Y, Lai Y, et al. CCoAOMT positively regulates the biosynthesis of secondary metabolites in *Zanthoxylum armatum*. Frontiers in Agronomy, 2025, 7:1604811.

[11] Peiqin L, Zhao R, Zhaoxue F, et al. Integrated Transcriptome and Metabolome Analysis Revealed That Flavonoid Biosynthesis May Dominate the Resistance of *Zanthoxylum bungeanum* against Stem Canker..Journal of agricultural and food chemistry,2021,69(22):6360-6378.

[12] Han S, Xu X, Yuan H, et al.Integrated Transcriptome and Metabolome Analysis Reveals the Molecular Mechanism of Rust Resistance in Resistant (Youkang) and Susceptive (Tengjiao) *Zanthoxylum armatum* Cultivars.International Journal of Molecular Sciences,2023,24(19):14761.

[13] Yang X, Wang Y, Sun Y, et al. Integrated transcriptomics and metabolomics revealed the role of the flavonoid pathway in the resistance of *Zanthoxylum bungeanum* against leaf rust.Scientia Horticulturae, 2025, 341:113990.

[14] Wang Y, Shao Y, Zhao X, et al. High-efficiency fungicide screening and field control efficacy of maize southern corn rust. Crop Protection, 2025, 187:106997.

[15] Belan L L, Junior J C W, Souza F A, et al. Monitoring of leaf rust in conilon coffee clones to improve fungicide use. Australasian Plant Pathology, 2015, 44(1):5-12.

[16] Lei L, Dakuan Q, Ruixin Z, et al. Research on the Influence of Education of Farmers' Cooperatives on the Adoption of Green Prevention and Control Technologies by Members: Evidence from Rural China. International Journal of Environmental Research and Public Health, 2022, 19(10):6255.

[17] Qiong W, Shujie G, Xulong W, et al. Research on the Impacts of Information Capacity on Farmers' Green Prevention and Control Technology Adoption. Ecological Chemistry and Engineering S, 2022, 29(3):305-317.

[18] Hui S,Qing X, Zhangjie Z, et al. Disruption of the Novel Small Protein RBR7 Leads to Enhanced Plant Resistance to Blast Disease. Rice (New York, N.Y.), 2023, 16:42.

[19] Rouf R M, Sachin R, YuanMing Z, et al. Multi-faceted approaches for breeding nutrient-dense, disease-resistant, and climate-resilient crop varieties for food and nutritional security. Heredity, 2022, 128(6):387-390.

[20] Hu Y H, Zhou P, Mon S W, et al. TIDRE: An Efficient Tool for Isolating Antagonistic Endophytes and Screening Resistant Plants. Agriculture, 2025, 16(1):52-52.

[21] Wang M , Wang Y , Li X , et al. Integration of metabolomics and transcriptomics reveals the regulation mechanism of the phenylpropanoid biosynthesis pathway in insect resistance traits in *Solanum habrochaites*. Horticulture research, 2024, 11(2):277.

[22] Elhawary A E , Moussa Y A , Singab B N A . *Genus Curcuma*: chemical and ethnopharmacological role in aging process. BMC complementary medicine and therapies, 2024, 24(1):31.

[23] Gea G , Roberto B , Armando J M , et al. Production of Plant Secondary Metabolites: Examples, Tips and Suggestions for Biotechnologists. Genes, 2018, 9(6):309.

[24] Zeci L , Huiping W , Jianming X , et al. The Roles of Cruciferae Glucosinolates in Disease and Pest Resistance. Plants (Basel, Switzerland), 2021, 10(6):1097.

[25] Stephen J., Maximilian D., Cara N., et al. Modular terpene synthesis enabled by mild electrochemical couplings.Science, 2022, 375(6582):745-752.

[26] Cao Y., Liu L., Ma K., et al. The jasmonate-induced bHLH gene SlJIG functions in terpene biosynthesis and resistance to insects and fungus. Plant Biotic Interactions, 2022, 64(5):1102-1115.

[27] Wang W, Feng J, Wei L., et al. Transcriptomics Integrated with Free and Bound Terpenoid Aroma Profiling during "Shine Muscat" (*Vitis labrusca* × *V. vinifera*) Grape Berry Development Reveals Coordinate Regulation of MEP Pathway and Terpene Synthase Gene Expression. Journal of Agricultural and Food Chemistry, 2021, 69(4):1413-1429.

[28] Lu Z , Jiahao L , Yifei L , et al. Integrative metabolome and transcriptome analyses reveal the

molecular mechanism underlying variation in floral scent during flower development of *Chrysanthemum indicum* var. aromaticum . Frontiers in Plant Science, 2022, 13:919151.

[29] YongLiang X , Huan Y , Na L , et al. Increased production and anti-senescence activity of exopolysaccharides in Ganoderma lingzhi by co-overexpression of β-1,3-glucan synthase and UDP-glucose pyrophosphorylase. International journal of biological macromolecules, 2023, 253(P2):126778.

[30] Yang Y P , Xin M L , Jie W L , et al. DJ1 Ameliorates AD-like Pathology in the Hippocampus of APP/PS1 Mice. Biomedical and Environmental Sciences, 2023, 36(11):1028-1044.

[31] Yanyan T , Lin Z , Shanling G , et al. LncRNA LINC00974 Downregulates miR-122 to Upregulate RhoA in Oral Squamous Cell Carcinoma. Cancer biotherapy & radiopharmaceuticals, 2019, 36(1):18-22.

[32] Nicole R B , Graham J L . Grapevine mono- and sesquiterpenes: Genetics, metabolism, and ecophysiology . Frontiers in Plant Science,2023,14:1111392.

[33] Corral, J., Rocafort, M., Ripa, M.B. et al. The Ralstonia solanacearum catalase-peroxidase KatG is crucial to survive environmental stresses and also plays a role in plant infection. Sci Rep, 2025, 15:35168.

[34] Riseh S.R., Fathi F., Vatankhah M., et al. Catalase-associated immune responses in plant-microbe interactions: A review. International Journal of Biological Macromolecules, 2024, 280(P2):135859-135859.

[35] Wang S , Liu J , Zhou L , et al. Research progresses on mitochondrial-targeted biomaterials for bone defect repair. Regenerative biomaterials, 2024, 11:rbae082.

[36] Wang J, Cheng Y, Wang J, et al. Identification and validation of functional markers for the superoxide dismutase gene TaSOD-B2 in common wheat. BMC plant biology, 2025, 25(1):1481.

[37] Shen, C., Wang, Y. Recent Progress on Peroxidase Modification and Application. Appl Biochem Biotechnol 2024, 196: 5740–5764.

[38] Josinei F R, B V C, L A T I P, et al. Effects of Iron on oxidative stress of Cecropia hololeuca and Carica papaya plants. Anais da Academia Brasileira de Ciencias, 2022, 94(suppl 3):e20211098.

[39] Chen G , Zhang D , Chen F , et al. Uncovering the molecular mechanisms of *Acer fabri* in adjusting to low-temperature stress through integrated physiological and transcriptomic analysis. Scientific Reports, 2025, 15(1):3036.

[40] Zhang X , Zhang J , He J , et al. Physiological and Transcriptome Responses of *Pinus massoniana* Seedlings Inoculated by Various Ecotypes of the Ectomycorrhizal Fungus

Cenococcum geophilum during the Early Stage of Drought Stress. Journal of Fungi, 2024, 10(1):71.

[41] Liu S , Dai L , Qu G , et al. Integrative transcriptome and WGCNA analysis reveal key genes mainly in response to Alternaria alternata in *Populus simonii* × P. nigra.Frontiers in Plant Science, 2025, 16:1540718.

[42] Li Y , Xingxing W , Fuyong Z , et al. Roles of S-Adenosylmethionine and Its Derivatives in Salt Tolerance of Cotton. International journal of molecular sciences, 2023, 24(11):9517.

[43] Jiajia L , Lei W , Feng L , et al. Genome-wide identification, characterization and gene expression of BES1 transcription factor family in grapevine (*Vitis vinifera* L.). Scientific reports, 2023, 13(1):240-240.

[44] Penghua G , Ying Q , Lifang L , et al. *Amorphophallus muelleri* activates ferulic acid and phenylpropane biosynthesis pathways to defend against *Fusarium solani* infection. Frontiers in plant science, 2023, 14:1207970.